Long-term prediction of reinforced concrete structures - Use of thermodynamic data to assess steel corrosion in carbonated concrete

Bruno HUET[a,b,*], Valérie L'HOSTIS[a], Patrick. LE BESCOP [a], Hassane IDRISSI [b]

[a] Laboratoire d'Etude du Comportement des Bétons et Argiles, DEN/DPC/SCCME/LECBA, Bât. 158, CEA Saclay, 91191 Gif sur Yvette cedex, France, Huet@azurite.cea.fr
[b] Laboratoire de Physico-Chimie Industrielle (LPCI), INSA de Lyon, Bât. Léonard de Vinci, 20 av. Albert Einstein 69621 Villeurbanne cedex, France

Abstract

In the context of the prediction of the long-term behaviour of reinforced concrete structures involved in the nuclear waste storage, the corrosion mechanisms of the steels have to be assessed and modelled. When nuclear wastes are embedded in reinforced concrete containers, the chemical environment of the reinforcement is progressively modified, due to the diffusion of the carbonation front inside the concrete matrix. This modification leads to the variation of the properties of the iron oxides formed at the steel/concrete interface, and the active corrosion can be initiated.

In order to understand and modelled the mechanisms of steel corrosion in concrete, the equilibrium of two main systems must be separately described with the help of thermodynamic data issued from the literature:

• The mineral phases, lime and calcium silicate hydrate (C-S-H), in equilibrium with the pore solution during the propagation of the carbonation front,
• The iron oxides in equilibrium with the aqueous solution.

For this purpose, the nature of aqueous species present in the pore solution was calculated in the whole range of pH encountered during the cement paste degradation by carbonation. As a matter of fact, as the pH decreases, calcium concentration decreases and silicates concentration increases due to the calcium carbonate formation and C-S-H dissolution. The pH of a carbonated concrete ranges between 8.3 and 10, depending on the partial pressure of carbon dioxide in the porosity and the conversion degree of carbonation. In this pH range, the iron oxides equilibria were analysed as a function of the redox potential and aqueous species (carbonates and sulphates present in the solution) present inside the solution. In a reductive solution and in presence of carbonates, the high solubility of iron oxides may prevent passivation or generate the dissolution of the passive film.

Moreover, the relevance of thermodynamics calculations has been confirmed by corrosion tests of mild steel immersed in solutions containing carbonates, in the pH range 8.3 to 10.

Keywords: low alloyed steel, corrosion in concrete, modelling, long term prediction

1 Introduction

Reinforced concrete is a structure material largely used in the french nuclear industry, for nuclear plants, and for nuclear waste storage. Steel reinforcement is used to improve the tensile strength of concrete structures.

In the case of nuclear waste storage, reinforced concrete structures provide not only improved mechanical properties but also the confining of radionucleides. The growth of cracks in concrete would alter its confining properties. The cracking of concrete can be due to chemical degradation, frost/thaw cycles, wetting/drying cycles or corrosion of reinforcement.

Non-alloyed or low alloyed carbon steel is often used as reinforcement in these structures. Thanks to the high pH of the concrete interstitial solution, reinforcement remains at a passive state. Very low corrosion rate are measured and no mechanical degradation is generated. Unfortunately, concrete is a porous material which may react with the surrounded media. Especially, the atmospheric carbon dioxide generates carbonation of concrete. Carbonation alters physical and chemical properties (pH decrease) of concrete. Moreover, in carbonated concrete, the corrosion state of the rebar does no longer remain in its passive state and high corrosion rate can be evaluated. The growing of new iron oxides at the steel concrete interface generates tensiles stresses in the carbonated concrete which may lead to the cracking. Thus, the time evolution of the steel concrete interface is often schematized by the diagramm of Tuutti [1].

2 Corrosion modelling: state of the art

Investigations on the electrochemical and corrosion behaviour of iron immersed in alcaline solutions (NaOH, KOH 0,1 M to 1 M) have highlighted its very low oxydation kinetic [2,3,4]. The passive oxide layer remains very thin [5] and can not lead to the cracking of concrete. Chemical degradation of concrete (leading to high corrosion rate of the rebar) is necessary for cracking occurence.

The chemical degradation of concrete due to chloride ingress or carbonation is well known. Moreover, the depassivation conditions in terms of chloride concentration or pH decrease have been subject to a lot of investigation [6,7,8]. Thus, the time to depassivation may be predicted with an almost good accuracy.

A lot of experimental data are disponible on the corrosion rate of steel reinforcement in degraded concrete. However, no literature was found about the mechanistic modelling of reinforcement corrosion in carbonated concrete. Some mechanistic models do exist but most of the time, they describe mild steel corrosion in other aqueous environnements.

Three kinds of model may be used to predict the long term evolution of corrosion [9]: a material balance approach, semi empirical approach or mechanistic modellling. However, the mechanistic modelling is the only method which can be extrapolated to very long time which can not be reached in laboratory experiments.

The mechanistic models are based on the integration of elementary mechanisms in analytical or numerical model. Those models requires the implementation of kinetic reaction constants, diffusion constants, dissolution constant which are not mentioned in the literature. The evolution laws deduced from those models may be then compared to semi-empirical law evaluated from laboratory tests.

A few authors have tried to model iron corrosion in degraded concrete [10,11]. They all propose to evaluate corrosion rate with the Butler-Volmer activation law. This law permits to evaluate corrosion rate as a function of the anodic and cathodic overpotentials and Tafel coefficient. Nevertheless, those models do not take into account the aqueous transport of

reactive species in the porosity of degraded concrete. Actually, the reaction kinetics at the interface may not be the controlling factor of the corrosion rate.

For example, the corrosion modelling of mild steel in deep reductive clays is based on a dense corrosion layer between metallic substract and the clay. In this particular case, the growing of the oxides layer is limited by species motion in the solide phase: electron or point default motion (anionic or cationic) [12,13].

In the case of atmospheric corrosion of low alloyed steels during the storage, the wetting and drying cycles have been identified as critical to evaluate the metal loss over time. In particular, the oxygen reduction during the wet period leads to high metal loss. The reduction of oxygen has been modelled assuming the electrical conductivity of the porous oxide layers. The transport of oxygen in a thin water layer on the iron oxides is the limiting step of the system [14,15].

3 Mechanistic modelling of corrosion in carbonated concrete

This section presents the basis of a new mechanistic model for rebar corrosion in carbonated concrete. The model is based on the analysis of ancient ferrous artefacts and laboratory experiments performed on mild steel immersed in carbonated solution. Actually, investigation on ancient ferrous artefacts embedded in carbonated binders have shown a structuring of the oxides at the steel concrete interface [16,17], this oxide being porous, even in the vicinity of the iron substract [18]. Corrosion tests of mild steel immersed in carbonated solution have shown a structuring of the born oxides at the steel concrete interface into two layers. This basis layer is adhesive to the substract and the upper layer is less-adhesive [19].

The model will be structured upon the latter observations on two units (Fig. 1):

1. The first unit will describe the formation of iron oxides by co precipitation of the ferrous/ferric cations couple to the transport by diffusion of aqueous species, in the carbonated concrete [20]. In this part of the model, the local chemical equilibrium of mineral phases is considered to be always respected.
2. The second unit will describe the corrosion of the iron substract in the presence of a porous and thin oxide basis layer. In this case a local chemical disequilibrium will be assumed. Then reaction kinetics will be therefore introduced.

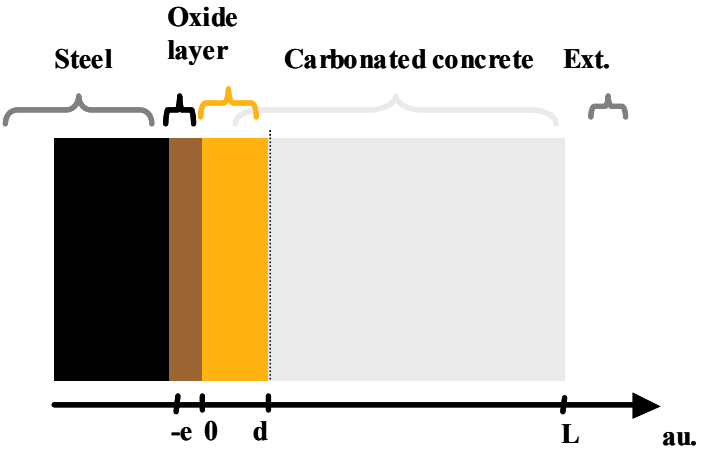

Figure 1 : Schematic representation of the corroding steel concrete interface.

3.1 Unit 1: Reactive transport modelling of iron aqueous species

Reactive transport modelling is largely used for geological application. The coupling of geochemical reaction and hydrogeological processes such as transport by diffusion, integrated in a numerical model, allows, for example, the prediction of the release of nuclear waste in clay or concrete barriers [21]. Moreover, those numerical models have been

successfully used for aqueous degradation of hydrated cement paste [22,23]. Nevertheless, those models, applied to corrosion of mild steel in soil or carbonated concrete, are new and usefull tools to predict the decrease of the total concrete porosity in the vicinity of the steel/mineral barrier interface [24].

Before using hydrogeochemical model, the description of the chemical equilibrium of mineral phases is necessary. In the $CaO\text{-}SiO_2\text{-}H_2O$ system, calcium silicates hydrates precipitate for a calcium aqueous concentration greater than ≈ 1 mmol/L. In presence of C-S-H, the pH is set by the ratio $[Ca]_{aq}/[Si]_{aq}$. The pH ranges from 10 for low Ca/Si ratio (≈0.8) to 12.5 for high Ca/Si ratio (1.8) [25].

The introduction of carbon dioxide in the porosity of concrete leads to the lime dissolution ($Ca(OH)_2$) and decalcification of calcium silicates hydrates (C-S-H).

$$Ca(OH)_2 + CO_2 \Rightarrow CaCO_3 + H_2O$$

In the $CaO\text{-}H_2O\text{-}CO_2$ open system, the pH is fixed by the presence of calcium carbonate ($CaCO_3$) and the partial pressure of carbon dioxide. In the atmosphere, $pCO_2 = 0.3$ mbar and the resulting pH is around 8.3.

In a wide pH range, the pH of the interstitial solution is fixed by the mineral phases of the hydrated cement paste. The formation reaction of iron oxides depends on the pH as weel as on the redox potential of the solution. In our case, the $CaO\text{-}H_2O\text{-}CO_2$ open system set the pH value (8.3). Thus the solubility of iron oxides does only depend on the redox potential of the aqueous solution, this is the ferric to ferrous cations ratio. For example, the formation reaction of siderite, magnetite and goethite can be written:

$$Fe[^{2+}] + HCO_3[^-] \Rightarrow FeCO_3 + H[^+]$$

$$Fe[^{2+}] + 2\,Fe[^{3+}] + 4\,H_2O \Rightarrow Fe_3O_4 + 8\,H[^+]$$

$$Fe[^{3+}] + 2\,H_2O \Rightarrow FeOOH + 3\,H[^+]$$

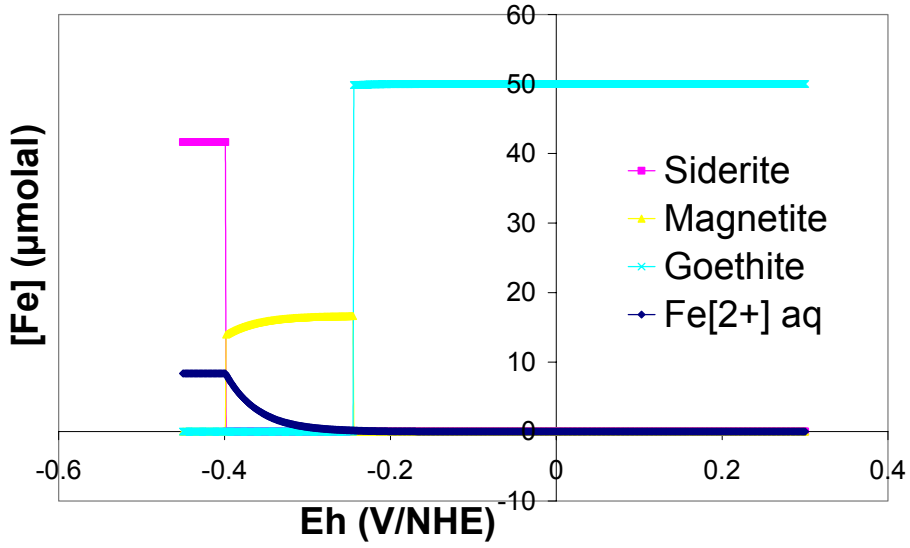

Figure 2: Nature of iron oxides at thermodynamic equilibrium as a function of redox potential. $[Fe]_{tot}$ = 50 µmolal, pH = 8.3, pCO_2 = 0.3 mbar. Thermodynamic data selected in reference [26].

As shown on figure 2, siderite is the most stable oxide in a reductive solution (Eh < -400 mV/NHE). For less reductive solutions, magnetite is the most stable phase (-400

mV/NHE < Eh < -250 mV/NHE). In oxidizing solution, iron is completely converted into goethite [26,27].

Even in reductive solutions, the aqueous concentration of ferrous ions in equilibrium with siderite is very low (≈ 10 µmolal). Moreover, the higher is the redox potential of the solution, the smaller is the concentration of aqueous iron. For redox potential values over -400 mV/NHE, iron is completely converted into magnetite or goethite, thus the aqueous concentration of iron can be neglected. However, complexation reaction of iron by carbonates increases the concentration of aqueous iron.

With a pertinent knowledge of the iron speciation in degraded concrete interstitial solution, the 0-D (0 dimensionnal) iron chemistry in carbonated water can be coupled to transport species through interstitial solution. The flux of iron species in concrete porosity and the oxide formation in the porosity may be evaluated by means of numerical models [21]. Moreover, those models take into account the variation of the porosity and the effective diffusion coefficient. Results of reactive transport modelling of iron in degraded concrete will be presented in a next paper.

3.2 Unit 2: Corrosion modelling

The aim of this section is to identify the limiting step of iron corrosion in presence of a thin (micrometric) and porous basis layer. There are two kinds of limiting steps : reaction kinetics or species transport. Here is considered anionic and cationic transport through capillar porosity of the iron oxides and electron motion through solid phase depending on its conductivity (Fig. 3). The reduction of oxygen and the formation of iron oxide are considered as reactions controlled:

$$O_2 + 2\,H_20 + 4\,e^- \Rightarrow 4\,OH^-$$

$$Fe^{2+} + 2\,OH^- \Rightarrow Fe(OH)_2$$

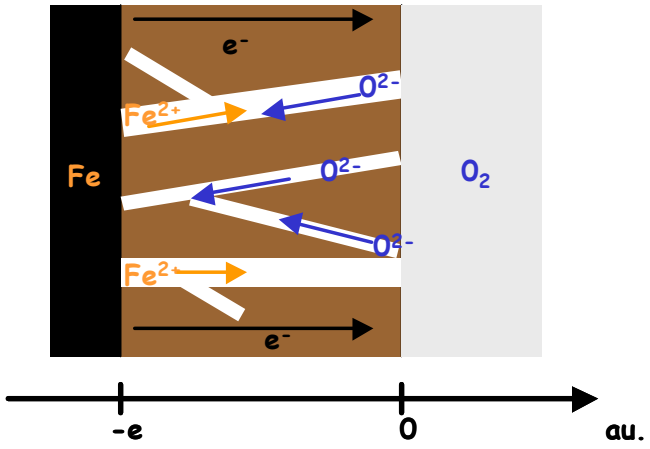

Figure 3: Schematic representation of elementary mechanism for the growing of the iron oxides layer.

3.2.1 Cathodic reaction

In this section, the cathodic reduction current density is evaluated. The following hypotheses are drawn before calculation:

- The saturation degree of concrete is below 0.9. Thus, the oxygen permeability of concrete is sufficient to maintain oxidising conditions at the oxide/concrete interface.
- The oxide layer is water saturated. Actually, the porosity of the oxide is in the nanometric scale [18] and permits water condensation.

- The porosity of concrete is described by a simple net of tortuous capillary.
- The properties of the oxide layer are homogen in the whole layer (porosity, specific surface).
- All transport mechanisms are in stationnary state.
- The oxygen reduction follows a 1st order reaction kinetic and can be written as follow :

(1) $$V(x) = k\,c(x)$$

- Two cases are then considered depending on the electrical conductivity or the iron oxide :

Case I : The oxide layer is not an electrical conductor. This is the case of the most oxides or oxi-hydroxides which are semi-conductive (n or p) with a band gap around 2 eV [20]. Oxygen is then reduced at the steel/oxide interface.

Case II : The oxide layer is considered as an electrical conductor. This is the case of magnetite which is semi-conductive with a little band gap of 0.1 eV [20]. Thus magnetite becomes conductive under low thermal activation. Then, reduction of oxygen may take place in the whole oxide layer, on its pores surface. Anodic and cathodic reactions take place on opposite reaction sites.

3.2.1.1 Case 1: Non-conductive oxide layer.

In the case of a non-conductive oxide layer, the one dimensional mass balance equation, applied to oxygen in an elementary volume, can be written as follow:

(2) $$\frac{\partial c}{\partial t} = 0 = \frac{\phi}{\tau} D \frac{\partial^2 c}{\partial x^2}$$

The latter equation can be solved with the next boudary conditions:

(3) $$c = c_0 \text{ at } x = 0$$

(4) $$-j_{diff} = \frac{\phi}{\tau} D \frac{\partial c}{\partial x} = k\,\phi\,c_L \text{ at } x = L$$

Thus, the oxygen concentration profile in the oxide layer can be evaluated:

(5) $$c = c_0 \left(1 - \frac{1}{1 + \frac{D}{\tau L k}} \frac{x}{L} \right)$$

and the oxygen reduction current density can be calculated:

(6) $$i = n F \phi k c_0 \frac{1}{1 + \frac{\tau L k}{D}}$$

with
- c oxygen concentration at x ($mole/m^3_{sol}$),
- c_L oxygen concentration at x = L ($mole/m^3_{sol}$),
- c_o dissolved oxygen concentration imposed by the Henry's law ($2{,}4\ 10^{-4}$ mol/l under $pO_2 = 0{,}2$ bar).
- k kinetic constant of oxygen reduction ($\approx 10^{-5}$ m/s),
- D oxygen diffusion coefficient in water ($1{,}9\ 10^{-9}$ m²/s),
- ϕ total porosity of the oxide layer (between 0,1 et 0,3),
- τ tortuosity (≈ 3),
- n amount of electron involved in the reaction (= 4),
- F Faraday constant (96500 C/mole),
- j_{diff} oxygen flow.

Equation (6) indicates that the oxygen reduction current density depends on the value of the ratio $\tau L k / D$. Depending on its value, cathodic reaction is under reactive, dual or diffusion control. A numerical application is shown on figure 4:

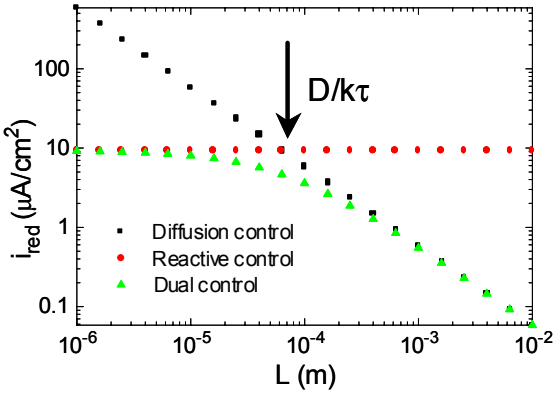

Figure 4: oxygen reduction current density as a function of oxide layer thickness : illustrating the three cases of kinetic control.

The cathodic current density is under diffusion control only when the thickness is greater than the critical length D/kτ. Below this critical value, oxygen reduction is under reactive control. As the layer thickness is supposed to range in the micrometric scale [16], the corrosion process should not be under oxygen diffusion control but under reactive control.

3.2.1.2 Case 2: Conductive oxide layer.

In the case of a conductive oxide layer, the one dimensional mass balance equation, applied to oxygen in an elementary volume, can be written as follow:

(7) $$\phi \frac{\partial c}{\partial t} = 0 = \frac{\phi}{\tau} D \frac{\partial^2 c}{\partial x^2} - s_a k \phi c$$

(8) $$\text{with } s_a = (1-\phi)\rho S_a$$

ρ oxide density (kg/m^3),
S_a specific surface (m²/g),
s_a specific surface (3,7 10^7 m^2/m^3 [18]).

The mass balance equation is a 2nd order differential equation, that can be simplified as follow:

(9) $$\lambda^2 \frac{\partial^2 c}{\partial x^2} - c = 0$$

(10) $$\text{with } \lambda = \sqrt{\frac{D}{\tau s_a k}}$$

Equation 9 is solved in the case of a half infinite oxide layer. At the oxide/concrete interface the oxygen concentration is c_0. Thus the oxygen concentration profile in the oxide layer can be evaluated:

(11) $$c = c_0 \exp\left(-\frac{x}{\lambda}\right)$$

and the oxygen reduction current density can be calculated by integration of the local current density on the whole oxide layer

(12) $$i = n F s_a k \lambda \phi c_0$$

From the latter equations (11 and 12) and the numerical application, the following assessments can be drawn:

- λ is the characteristic length on which oxygen is reduced. λ is a function of oxide layer properties (D, s_a) and kinetic constant. As λ is small ($\lambda \approx 1$ µm), equation 12 indicates that oxygen reduction is under reactive control.
- the oxygen reduction current density value is 200 µA/cm². This valus is $s_a\lambda$ (≈20) greater than the one evaluated for the non-conductive oxide layer (under reactive control). The porous oxide layer increases the total surface on which oxygen is reduced.
- 5λ down the external surface, the oxygen concentration is $c_0/100$.

The validity domain of the model is limited by the following points:

- The model cant not be applied to describe the initial stages of corrosion because the thickness of the new born oxide layer is smaller than the caracteristic length λ. Thus, the initial surface state of the rebar is of major importance.
- The model does not take into account heterogeneities in the oxide layer that could induce preferential transport path.
- The oxygen reduction current density does not depend on the oxide layer thickness. Thus the corrosion rate should not decrease over time. This result is in contradiction with the general assumption that corrosion rate decreases with aging of the sample. Actually, corrosion rates usually follow a logarithm law : $I = k\, t^{-n}$
- The model disregards the induced increase of the pH. Actually, a pH increase reduces solubility of the oxide. Thus, the porosity should decrease in the oxygen reduction zone.

3.2.2 Anodic reaction

The same mass balance equation as (9) may be applied to the formation of ferrous hydroxide under the following assumptions:

- The formation reaction of ferrous hydroxide $Fe(OH)_2$ does only depend on the concentration of ferrous cations. The supply of hydroxide ions should be sufficient.
- The flow of aqueous ferrous cations at $x = -e$ is set by the oxygen reduction.
- The mass balance equation is solved for a half infinite oxide layer.

Thus, the solution of the mass balance equation can be written:

$$C(x) = \frac{I_{O2}}{nFS}\frac{\lambda}{D_a}e^{\left(-\frac{x}{\lambda}\right)} \qquad (13)$$

Assuming a kinetic constant in the same order of magnitude as for the reduction of oxygen, the ferrous hydroxide formation takes place in the same characteristic length λ from the steel/oxide interface. The mineral formation leads to a decrease of the porosity in the vicinity of the rebar. The model does not take into account any spatial or time distribution of the porosity. However, the critical length λ decreases with the total porosity of the oxide layer (see equation 13 and 10). Thus, after a few time step, the precipitation of oxide should lead to the formation of a dense oxide acting as an diffusion barrier.

The calculation takes into account only ferrous cations in solution, all other species concentration being fixed. It means that the diffusion coefficient of ferrous cations is far smaller than those of other aqueous species. Nevertheles, the mobility of aqueous species is very similar. Thus there is no reason to attribute different diffusion coefficient to each species.

Anodic and cathodic reaction does not take place on the same reaction sites. At the steel/oxide interface, ferrous cations are formed and at the opposite oxide/concrete interface hydroxide ions are produced. Thus, a potential gradient appears due to the charge space distribution. The motion of ions in the solution should be solved with the Nernst Planck equation, which takes into account the potential gradient on ionic transfert.

4 Conclusion

The long term prediction of the corrosion of reinforcement in carbonated concrete needs the understanding and modelling of the iron oxide formation at steel concrete interface. Actually in the literature, only short terms laboratory experiments are presented and no mechanistic model of reinforcement corrosion has been established. In this paper, the basis of a mechanistic model has been constructed on two units. The first unit described the speciation of iron in carbonated concrete solution, assuming the local equilibrium. Depending on the redox potential, siderite ($FeCO_3$), magnetite (Fe_3O_4) and goethite (α-FeOOH) should precipitate. The low solubility of those oxides, even in a reductive media, should limit the transfer of iron aqueous species in solution. The second unit aims to evaluate the corrosion rate of the reinforcement in presence of a thin and porous oxide layer, assuming the local disequilibrium. Calculations have shown that the corrosion rate should not be under cathodic control, whatever the conductivity of the iron oxides is, but under anodic control. Actually, iron oxide precipitation should lead to the formation of a dense diffusion barrier layer.

1 K. Tuuti, « Corrosion of Steel in Concrete », Swedish Cement and Concrete Research Institute, 1982

2 D.D. MacDonald, B. Roberts, The cyclic voltammetry of carbon steel in concentrated sodium hydroxide solution, Electrochimica Acta, 1978, 23, 781-786.

3 R. Grauer, B. Knecht, P. Kreis, J.P. Simpson, “Die Langzeit-Korrosiongeschwindigkeit des passiven Eisens in anaeroben alkalischen Lösungen”, Werkstoffe und Korrosion, 1991, 42, 637-642.

4 S. Joiret, M. Keddam, « Use of EIS, ring-disk electrode, EQCM and Raman spectroscopy to study the film of oxides formed on iron in 1 M NaOH », Cement and Concrete Research, 2002, 24, 7-15.

5 P. Schmuki, M. Büchler, H. Böhni et al, “Passivity of Iron in alkaline solutions studied by in situ XANES and a Laser reflection technique”, Journal of the Electrochemical Society, 1999, 146, 2097-2102.

6 W. Breit «Kritischer Chloridegehalt-Untersuchungen an Stahl in chloridhaltigen alkalischen Lösungen», Materials and Corrosion, 1998, 49 , 539-550

7 C. Alonso, M. Castellote, C. Andrade “Chloride threshold dependence of pitting potential of reinforcements”. Electrochemica Acta, 2002, 47, 3469-3481

8 M.A. Climent, C. Gutiérrez. « Proof by UV-visible modulated reflectance spectroscopy of the breakdown by carbonation of the passivating layer on iron in alkaline solution ». Surface Science. 1995, Vol. 330, 651-656.

9 ANDRA, Référentiel matériaux, novembre 2001

10 I. Petre-Lazar, « Evaluation du comportement en service des ouvrages en béton armé soumis à la corrosion des aciers – Outil d’aide à la décision », Thèse de l’université de Laval, novembre 2000.

11 Z.P. Bažant, « Physical model for steel corrosion in concrete sea structures – Application », Journal of the structural division, 1979, 1155-1166.

12 C. Bataillon, « Corrosion modelling of iron based alloy in neutral media », Eurocorr 2004, Nice

13 D.D. MacDonald, “The point defect model for the passive state”, Journal of the Electrochemical Society, 1992, 139, 3434-3449.

14 S. Hoerlé, F. Mazaudier, Ph. Dillmann, G. Santarini, « Advances in understanding atmospheric corrosion of iron. I. Rust characterisation of ancient ferrous artefact exposed to indoor atmospheric corrosion ». » Corrosion Science, 46, (2004), 1401-1429

15 M. Stratmann, J. Müller, « The mechanism of the oxygen reduction on rust covered metal substrates ». Corrosion Science. 1994, Vol. 36, 327-359.

16 W.J. Chitty, P. Dillmann, V. L’Hostis, C. Lombard, Long term corrosion resistance of metallic reinforcements in concretes – A study of corrosion mechanisms based on archaeological artefacts (submitted to Corrosion Science, 2004).

17 W.J. CHITTY, P. DILLMANN, V. L'HOSTIS, G. BERANGER, On the characterisation of the corrosion layout of ferrous archaeological analogues in binders, proceedings of the Eurocorr 2004 conference, Nice, France (12-16 septembre 2004).
18 Ph. Dillmann, F. Mazaudier, S. Hoerlé, « Advances in understanding atmospheric corrosion of iron. II. Mechanistic modelling of wet-dry cycles. » Corrosion Science, 46, (2004), 1431-1465
19 B. Huet, V. L'Hostis, H. Idrissi, G. Santarini, D. Féron, « Étude des cinétiques de corrosion d'un acier doux en milieu cimentaire – Expérimentations et modélisation » Journées d'Etude de la Cinétique Hétérogène, CEA Saclay, mars 2003.
20 R.M. Cornell, U. Schwertmann, « The Iron Oxides », WILEY-VCH, 2nd Edition, 2003, 664 p.
21 J. van der Lee, L. de Windt, "Present state and future directions of modeling of geochemistry in hydrogeological systems", J. Contaminant Hydrology, 47, 2001, 265-282
22 D. Planel, « Les effets couplés de la précipitation d'espèces secondaires sur le comportement mécanique et la dégradation chimique des bétons », thesis of University Marnes-la-Vallée, 2002
23 C. Gallé, H. Peycelon, P.Le bescop, « Use of cement-based materials for radioactive waste management: Comparative study of OPC, BFS-PFA and HFSC cement pastes leaching behaviour », 5th International Symposium on Cement and Concrete – Shanghai, 2002.
24 L. Trotignon, M.-H. Faure, M. Cranga, H. Peycelon, '"Numerical simulation of the interaction between granitic groundwater, engineered clay barrier and iron canister", Sci. Basis Nucl. Waste Manage.
25 R. Barbarulo, « Comportement des matériaux cimentaires : action des sulfates et de la température », Thesis of University of Laval and Ecole Normale Supérieure de Cachan, September 2002
26 J. Chivot, « Thermodynamique des produits de corrosion », ANDRA, February 2004
27 D. Neff, S. Reguer, « Structural characterisation of corrosion products on archeological iron. An integrated analytical approach to establish corrosion forms », J. Raman Spectrosc., 2003.